Effect of particle inertia on the viscous-convective subrange

Christopher A. Jeffery*
Atmospheric Sciences Programme, University of British Columbia, 217 Geography, 1984 West Mall, Vancouver, British Columbia, Canada V6T 1Z2

(Received 1 October 1999)

The spectral scaling of inertial particles in isotropic, homogeneous turbulence is investigated. The particle density spectrum of the Elperin-Kleeorin-Rogachevskii small-scale correlation function [Phys. Rev. E **58**, 3113 (1998)] is derived and extended to larger scales. In the scale range $(13–60)\eta$, a peak in the spectrum is observed when the ratio of the energies in the compressible and the incompressible components of the particle's velocity is greater than 0.007 (Stokes number >0.15). The peak is a manifestation of the accumulation of inertial particles in regions of high strain and low vorticity. The size and location of the peak are compared qualitatively with measurements of particle intermittency (preferential concentration) from direct numerical simulations.

PACS number(s): 47.27.Qb, 47.40−x

I. INTRODUCTION

Recently, much attention has been given to a simple model of passive scalar advection by a velocity field with long-range spatial correlations but no memory. Interest in this so-called ''δ-correlated'' model stems from two fronts: first- and second-order statistics can be solved exactly and with complete mathematical rigor using path integral [1,2], functional [3,4], or parametrix [5,6] methods and, conversely, an explicit set of recursive equations for all higher-order moments can be derived and solved with an appropriate closure approximation. In particular, Kraichnan's closure by ''linear ansatz'' [7,8] has motivated a large number of studies in this field (see Ref. [9], Sec. IV) because it exhibits anomalous scaling behavior and provides a good testing ground for the capabilities of renormalization-group methods [10–13] and renormalized perturbation theory [14,15]. Recently, the δ-correlated model has also been used to assess the effect of compressibility [16,17] or particle inertia [18,19] on scalar statistics, the latter being driven, in part, by the phenomena of ''preferential concentration''—the accumulation of dense particles in regions of high strain and low vorticity in a turbulent flow—developed largely in the engineering community and reviewed in [20]. In this short work, the scalar spectrum of the second-order correlation function presented in [19] using the δ-correlated model is derived and extended to larger scales, and a more direct comparison is made with results from numerical studies of preferential concentration [21].

Although equations for the passive scalar covariance in a compressible velocity field have only recently appeared, the incompressible case has a long history that can be traced back to the classical work of Richardson [22]. A diffusion equation for the second-order spatial correlations in a rapidly fluctuating velocity field has been repeatedly recovered in a number of papers [23–26] with varying expressions for the effective diffusivity, $D_{\mathrm{eff}}(\mathbf{x})$. The δ-correlated model can be derived formally by the velocity field renormalization $\mathbf{u}_\delta(t,\mathbf{x})=\delta^{-1}\mathbf{u}(\delta^{-2}t,\mathbf{x})$ where the molecular diffusivity D is not rescaled ($D_\delta=D$) and where the long time rescaling δ^{-2} is chosen to reproduce the conventional or normal diffusion $\langle\mathbf{x}^2(t)\rangle\sim t$ associated with a mean-field regime [27,28]. Under certain general conditions the random field $\mathbf{u}_\delta(t,\mathbf{x})$ converges to a white-noise process in the sense of distributions, i.e.,

$$\lim_{\delta\to 0}\langle\mathbf{u}_\delta(t+s,\mathbf{x}+\mathbf{r})\mathbf{u}_\delta(t,\mathbf{x})\rangle=2\tau\delta(s)\langle\mathbf{u}_\delta(\mathbf{x}+\mathbf{r})\mathbf{u}_\delta(\mathbf{x})\rangle, \tag{1}$$

where τ is the renewal time and $r\ll l_0$ where l_0 is the integral length scale. It is important to emphasize that this renormalization is not a uniformly valid theory in the large-scale limit ($r\to l_0$) because of the strong infrared divergence in the $k^{-5/3}$ Kolmogorov velocity spectrum, and therefore D_{eff} obtained under this rescaling should not be interpreted as an eddy diffusivity. From the renormalization above, it follows trivially that the rescaled Eulerian correlation time $\lim_{\delta\to 0}\tau_E\sim\delta^2$ is much less than the molecular diffusion time, and therefore this renormalization corresponds to the limit $\mathrm{Pr}\gg 1$, where the Prandtl number $\mathrm{Pr}=\nu/D$, and ν is the kinematic viscosity.

The correct renormalization in the large-scale limit for the δ-correlated model with Kolmogorov velocity statistics can be found by computing an effective time-rescaling function, $\rho^2(\delta)$, so that the ensemble average of the rescaled passive scalar field $\langle\psi_\delta(\mathbf{x}/\delta,t/\rho^2(\delta))\rangle$ has a nontrivial limit. This was done by Avellaneda and Majda [2], who found the superdiffusive scaling $\rho(\delta)=\delta^{2/3}$ and concluded that the eddy diffusivity D_* is unbounded, satisfying $D_*(\mathbf{r})\to\infty$ as $|\mathbf{r}|\to\infty$. Thus the second-order correlations are not well approximated by a simple Gaussian profile shape at large distances.

The diffusion equation obtained from the δ-correlated model was solved by Kraichnan [26] in the small-scale limit by expanding $D_{\mathrm{eff}}(r)$ to the first order in r^2. He derived k^{-1} viscous-convective scaling for the scalar spectrum with k greater than the Batchelor wave number in agreement with the earlier results of Batchelor [29]. Recently, both Bogucki *et al.* [30] and Chasnov [31] compared the Kraichnan and Batchelor models using direct numerical simulations and

*Electronic address: cjeff@geog.ubc.ca

found, unambiguously, that the Kraichnan or δ-correlated model is ''correct'' for $\mathrm{Pr}\gg 1$, in agreement with the analysis above. Elperin *et al.* [18] used the δ-correlated model to assess the effect of particle inertia on spatial statistics and found a mechanism for intermittency in particle concentrations (preferential concentration). They derived solutions for the nth-order correlation function Φ_n of the form $\Phi_n(t,\mathbf{r}) = \Pi_{i,j}^{n}\Phi_2[\mathbf{x}^{(i)}-\mathbf{x}^{(j)}]\exp[0.5n(n-1)\gamma_2 t]$ where $i\neq j$, from which it follows that if the second moment of the particle concentration grows ($\gamma_2>0$), then so do all higher-order correlation functions. A Reynolds number criterion for $\gamma_2>0$ was derived that, when satisfied, implies self-excitation of fluctuations in particle concentration without external pumping, and thus intermittency. In a later work, Elperin *et al.* [19] presented a steady-state solution for $\Phi_2(\mathbf{r})$ in the small-scale regime, r less than the Kolmogorov length $\eta = (\nu^3/\varepsilon)^{1/4}$, where ε is the energy dissipation rate, and found that anomalous scaling appears when the degree of compressibility $\sigma>1/27$.

In these studies of particle inertia using the δ-correlated model, implicit and explicit assumptions (e.g., $\mathrm{Pr}\gg 1$) have been made. First consider the molecular diffusivity D. The Kraichnan model, derived in [26] assuming a continuous particle field, gives a spectral decay of the form $\exp(-\eta_B k)$ where $\eta_B=(D\tau_\eta)^{1/2}$ is the Batchelor length and $\tau_\eta = (\nu/\varepsilon)^{1/2}$ is the Kolmogorov time. Using Einstein's relation $D\sim d_*^{-1}$, where d_* is the particle diameter, $\eta_B\to 0$ as $d_*\to\infty$, from which it follows that the spectral decay is incompatible with the particle radial distribution function for $\eta_B<d_*$. Thus to correct for finite particle size in what follows, an effective diffusivity defined by $\tilde{D}=\max(D,d_*^2\tau_\eta^{-1})$ is used, where the tilde has been dropped. Furthermore, using $\mathrm{Pr}\gg 1$ and the effective diffusivity, $d_*\ll\eta$ that is also a stated assumption in [19]. And finally, although the effect of particle inertia is considered where the particle density ρ_p is greater than the fluid density ρ_f, the particle mass loading $\alpha_p\rho_p/\rho_f$ where α_p is the volume fraction of particles is assumed to be small, implying an insignificant modulation of the turbulence, typically referred to as one-way coupling.

The paper is organized as follows. In Sec. II the covariance equation for inertial particle concentration first derived in [18] is discussed and the corresponding spectral equation for $\Phi_2(\mathbf{k})$ in the regime $k\gg\eta^{-1}$ presented and solved. Limitations of $\Phi_2(\mathbf{k})$ extrapolated into the regime $k\sim O(\eta^{-1})$ are presented in Sec. III, and in Sec. IV I derive a closed-form expression for $\Phi_2(\mathbf{k})$ that is accurate in this regime. Section V is a discussion of the effect of particle inertia on $\Phi_2(\mathbf{k})$; a number of figures are used for illustration and an explicit comparison is made with results from Wang and Maxey [21]. Section VI is reserved for conclusions.

II. SCALAR COVARIANCE EQUATIONS

The number density $n_p(t,\mathbf{x})\in\mathbb{R}_+=[0,\infty)$ of small particles in a compressible velocity field is described by the advection-diffusion equation

$$\frac{\partial n_p}{\partial t}+\nabla\cdot(n_p\mathbf{U})=D\Delta n_p, \tag{2}$$

where $\mathbf{U}=\mathbf{V}_p+\mathbf{u}$ is a random velocity field, $\mathbf{V}_p=\langle\mathbf{U}\rangle$ is the mean-particle velocity, and $D\in\mathbb{R}_+$ is the effective molecular diffusion coefficient discussed in Sec. I. Without loss of generality, we can consider the case $\mathbf{V}_p=0$ because of the Galilean invariance of Eq. (2). An equation for the second-order correlation function $\Phi_2\equiv\Phi=\langle\Theta(\mathbf{x})\Theta(\mathbf{y})\rangle$ can be constructed from Eq. (2) upon multiplication by $\Theta(\mathbf{y})$:

$$\frac{\partial\Phi}{\partial t}=2D\nabla^2\Phi-2\langle\nabla\cdot\{\mathbf{u}(\mathbf{x})[\Theta(\mathbf{x})\Theta(\mathbf{y})+N(\mathbf{x})\Theta(\mathbf{y})]\}\rangle, \tag{3}$$

where $\Theta=n_p-N$ and $N=\langle n_p\rangle$ is the mean number density of particles. First consider the incompressible case $\nabla\cdot\mathbf{u}=0$. Neglecting diffusion and averaging over an ensemble of Lagrangian trajectories for a given realization of $\mathbf{u}(t,\mathbf{x})$, the field $\Theta_u(t+\Delta t,\mathbf{x})$ can be written in terms of a Taylor series expansion of $\Theta_u(t,\boldsymbol{\xi}_{\Delta t})$ around $\mathbf{x}$ ([19], Appendix A):

$$\begin{aligned}\Theta_u(t+\Delta t,\mathbf{x})&=\langle\Theta_u(t,\boldsymbol{\xi}_{\Delta t})\rangle_{\boldsymbol{\xi}},\\ \Theta_u(t,\boldsymbol{\xi}_{\Delta t})&=\Theta(t,\mathbf{x})+\frac{\partial\Theta}{\partial x_m}(\boldsymbol{\xi}_{\Delta+}-\mathbf{x})_m+\cdots,\end{aligned} \tag{4}$$

where $\boldsymbol{\xi}_{\Delta t}$ are the Lagrangian paths

$$\boldsymbol{\xi}_{\Delta t}=\mathbf{x}-\int_0^{\Delta t}\mathbf{u}(t_\sigma,\boldsymbol{\xi}_\sigma)d\sigma, \tag{5}$$

$t_\sigma=t+\Delta t-\sigma$ and $\langle\,\rangle_{\boldsymbol{\xi}}$ is an ensemble average over $\boldsymbol{\xi}$ that, for a given realization of $\mathbf{u}(t,\mathbf{x})$, involves the averaging of $\mathbf{u}$ in the neighboring space $\boldsymbol{\xi}_{\Delta t}-\mathbf{x}$ and through future times Δt. Using the δ-correlated velocity field discussed in Sec. I, the ensemble averages $\langle\,\rangle$ in Eq. (3) and $\langle\,\rangle_{\boldsymbol{\xi}}$ in Eq. (4) become independent, and the Lagrangian and Eulerian statistics converge. Substituting Eqs. (4) and (5) into Eq. (3) and taking the limit $\Delta t\to 0$ in such a fashion that $\boldsymbol{\xi}_\sigma\to\mathbf{x}$ and $\int_0\mathbf{u}(t_\sigma)\mathbf{u}(t)d\sigma$ is finite [26] gives a diffusive term

$$\langle\nabla\cdot\{\mathbf{u}(\mathbf{x})[\Theta(\mathbf{x})\Theta(\mathbf{y})+N(\mathbf{x})\Theta(\mathbf{y})]\}\rangle=\langle\tau[u_m(\mathbf{x})u_n(\mathbf{x})-u_m(\mathbf{x})u_n(\mathbf{y})]\rangle\frac{\partial^2\Phi}{\partial x_m\partial y_n},$$

where τ is the momentum relaxation time from Eq. (1). Note that the δ-correlated in time random process yields Markovian behavior for the second-order statistics at all scales, although, in general, Eq. (4) includes non-Markovian effects.

For a compressible velocity field, Eq. (4) becomes the Feynman-Kac formula, which includes the characteristics $G_{\Delta t}=\exp[-\int_0^{\Delta t}b(t_\sigma,\boldsymbol{\xi}_\sigma)d\sigma]\approx 1-\int_0^{\Delta t}b(t_\sigma,\boldsymbol{\xi}_\sigma)d\sigma$ where $b=\nabla\cdot\mathbf{u}$ [19]. Evaluating the third term in Eq. (3) as above for $b\neq 0$ yields

$$\frac{\partial\Phi}{\partial t}=-2[D_{mn}(0)-D_{mn}(\mathbf{r})]\frac{\partial^2\Phi}{\partial x_m\partial y_n}+2\langle\tau b(\mathbf{x})b(\mathbf{y})\rangle\Phi-4\langle\tau u_m(\mathbf{x})b(\mathbf{y})\rangle\frac{\partial\Phi}{\partial x_m}, \tag{6}$$

where $\mathbf{r}=\mathbf{y}-\mathbf{x}$, and $D_{mn}=D\delta_{mn}+\langle \tau u_m u_n\rangle$. Equation (6) was initially derived by Elperin *et al.* [18] by first evaluating $\langle G_{\Delta t} n_p(t,\boldsymbol{\xi}_{\Delta t})\rangle_\xi$ along the Wiener path [19]:

$$\boldsymbol{\xi}_{\Delta t}=\mathbf{x}-\int_0^{\Delta t}\mathbf{u}(t_\sigma,\boldsymbol{\xi}_\sigma)d\sigma+(2D)^{1/2}\mathbf{w}(\Delta t), \tag{7}$$

where $\mathbf{w}(t)$ is a Wiener process, and then passing to the limit $\Delta t\to 0$ of $\partial\Phi/\partial t=[\Phi(t+\Delta t)-\Phi(t)]/\Delta t$. However, Eq. (6) in [18] contains the additional source term $I_2=2\langle \tau b(\mathbf{x})b(\mathbf{y})\rangle N^2$. The origin of this discrepancy can be elucidated by considering the scalar covariance equation constructed from Eq. (2) multiplied by $n_p(\mathbf{y})$. Deriving an equation for $\partial\langle n_p(\mathbf{x})n_p(\mathbf{y})\rangle/\partial t$ as per Eq. (6) for a homogeneous particle field and subtracting Eq. (6) leaves

$$\frac{\partial N(\mathbf{x})N(\mathbf{y})}{\partial t}=2\langle \tau b(\mathbf{x})b(\mathbf{y})\rangle N(\mathbf{x})N(\mathbf{y}). \tag{8}$$

Equation (8) should not be confused with the equation for $\partial N^2/\partial t$ that appears in [32], which must be derived from the equation for the mean field N. However, Eq. (8) does demonstrate that the term I_2 is best associated with a source of $N(\mathbf{x})N(\mathbf{y})$ and not Φ.

Particles with small but finite inertia have a velocity $\mathbf{U}\neq\mathbf{v}$ where $\mathbf{v}$ is the velocity of the surrounding fluid. Thus in the case in which $\mathbf{v}$ is divergenceless, homogeneous, and isotropic, $\mathbf{U}$ (or $\mathbf{u}$) will be compressible, homogeneous, and isotropic with the correlation function [16]

$$\langle \tau u_m(\mathbf{x})u_n(\mathbf{x}+\mathbf{r})\rangle=D_T\Bigg\{[F(r)+F_c(r)]\delta_{mn}+\frac{rF'}{d-1}\left(\delta_{mn}-\frac{r_m r_n}{r^2}\right)+rF_c'\frac{r_m r_n}{r^2}\Bigg\}, \tag{9}$$

where $F'=dF/dr$, $F(0)=1-F_c(0)$, and $D_T=u_0^2\tau/d$, where u_0 is the characteristic velocity of turbulent fluctuations with relaxation time τ, and d is the spatial dimension. The function $F(r)$ describes the solenoidal (incompressible) component of the longitudinal correlation coefficient, whereas $F_c(r)$ describes the potential (compressible) component.

Elperin *et al.* [19] solved Eq. (6) using Eq. (9) for $d=3$ in the viscous regime $r<\eta$. In this regime the correlation coefficients can be written as

$$F(r)=(1-\epsilon)[1-\alpha(r/\eta)^2],\quad F_c(r)=\epsilon[1-\alpha(r/\eta)^2], \tag{10}$$

where α is a constant and ϵ is a measure of the compressibility. The expression for $F(r)$ is accurate in the range $r\leqslant 5\eta$ estimated from the familiar Batchelor parametrization for the second-order structure function [33]. The corresponding expression for $F_c(r)$ is less accurate in the regime $r\sim O(\eta)$ because of the higher-order derivatives F_c'' and F_c''' that appear via $\langle \tau b(\mathbf{x})b(\mathbf{y})\rangle$ in Eq. (6). In Sec. IV, Eq. (10) for $F(r)$ is used with a more accurate expression for $F_c(r)$ that is also valid in the range $r\leqslant 5\eta$.

In order to recover the well-known viscous-diffusive regime in the limit $\epsilon\to 0$, it is appropriate to write $\alpha=f(\tau,u_0,\eta)$ and $\tau=g(|\gamma|)$ where $\gamma=-(1/q)\tau_\eta^{-1}$ is the average value of the least principal rate of strain, and q is a universal constant for high Reynolds number flows [29]. Recent numerical simulations suggest $q\approx 5.5$ [30,31]. The choice $\tau=|\gamma|^{-1}/6\approx\tau_\eta$ and $\alpha=\eta^2/(12\tau^2u_0^2)$ is consistent with both the well-known result $\alpha\approx\eta^2 d/(30\tau_\eta^2u_0^2)$ and the value of q in the viscous-convective regime giving $q=\sqrt{30}\approx 5.5$. The solution of Eq. (6) using Eq. (10) is [19]

$$\Phi(r)=\frac{1}{X}(1+X^2)^{\mu/2}S(X), \tag{11}$$

where $X=(\alpha\beta_m\mathrm{Pe})^{1/2}r$, $S(X)=\mathrm{Re}\{A_1P_\zeta^\mu(iX)+A_2Q_\zeta^\mu(iX)\}$; $P_\zeta^\mu(iX)$ and $Q_\zeta^\mu(iX)$ are the Legendre functions with imaginary argument $Z=iX$; $\beta_m=(1+3\sigma)/3(1+\sigma)$, $\mu=15\sigma/(1+3\sigma)$, $\zeta(\zeta+1)=\mu^2-5\mu+2$; $\mathrm{Pe}=u_0^2\tau/D\gg 1$ is the Péclet number, and the parameter of compressibility $\sigma=\epsilon/(1-\epsilon)$. Note that for an incompressible velocity field, $\sigma=0$, the correlation function for $0\leqslant r\ll(\alpha\mathrm{Pe})^{-1/2}l_0$ is $\Phi(r)=\mathrm{const}$, corresponding to the well-known k^{-1} viscous-convective scaling.

It is often useful to consider the spectral covariance density function $\Psi(\mathbf{k})=(2\pi)^{-d}\int d\mathbf{r}\,\Phi(\mathbf{r})\exp(-i\mathbf{k}\cdot\mathbf{r})$, where $\Psi\in\mathbb{C}$: $\mathrm{Re}\{\Psi\}\in\mathbb{R}_+$, $\Psi(\mathbf{k})=\Psi^*(-\mathbf{k})$, to gain some understanding of the relative contribution of individual wave numbers to the overall variance. Fourier transforming Eq. (6) [$\partial/\partial r_j\to ik_j, r_j\to i\partial/\partial k_j$] and using isotropic, viscous regime velocity correlation coefficients (10) as above yields a Bessel-type equation accurate for $k>\eta^{-1}$;

$$0=-\lambda^2k^2\Psi+k^2\Psi''+Bk\Psi'+C\Psi, \tag{12}$$

where $\Psi(k)\in\mathbb{R}_+$, $\lambda=[6D|\gamma|^{-1}(1-2\sigma/(1+3\sigma)]^{1/2}$ is a diffusive length scale ($\propto\eta_B$), $B=2[2+15\sigma/(1+3\sigma)]$, $C=120\sigma/(1+3\sigma)$, and the primes denote differentiation with respect to k. The spectral density $\Psi(k)$ may be obtained by solving Eq. (12) [34] or by Fourier transforming Eq. (11) directly giving

$$\Psi(k)=C_1k^\mu K_\nu(\lambda k)+C_2k^\mu I_\nu(\lambda k), \tag{13}$$

with $\{K,I,\mu\}\in\mathbb{R}$, $\nu\in\mathbb{C}$; and where I and K are modified Bessel functions, $\mu=(1-B)/2=-3/2-15\sigma/(1+3\sigma)$ and $\nu=[(1-B)^2-4C]^{1/2}/2=3/2[1-(100/3)\sigma/(1+3\sigma)^2]^{1/2}$. As per Eq. (11) discussed in [19], two qualitatively different regimes characterize the behavior of Eq. (13). For $\sigma\leqslant 1/27$, $\mathrm{Im}\{\nu\}=0$, $C_2=0$, and the scaling in the range $k\ll\lambda^{-1}$ is normal; i.e., $\Psi(k)\sim k^{\mu-\nu}$. On the other hand, for $\sigma>1/27$, $\mathrm{Re}\{\nu\}=0$ and the scaling is anomalous; i.e., $\Psi(k)\sim k^\mu\cos(|\nu|\ln k+\phi)$, where ϕ is an arbitrary phase. Furthermore, the presence of the additional parameter ϕ (i.e., $C_2\neq 0$) implies that the spectral transfer is nonlocal—given $\Psi|_{k_0}$ the spectral transfer $\partial\Psi/\partial k|_{k_0}$ is determined by a boundary condition that sets ϕ at some $k\ll k_0$ near the boundary of the inertial- and viscous-convective regimes. The nonlocal nature of the spectral covariance for $\sigma<1/27$ prevents the determination of C_1 and C_2 without resorting to a direct numerical simulation of Eq. (2) and, therefore, this regime is not considered further in this work. Note that for an incompressible velocity field $\sigma=0$, Eq. (13) reduces to the analytic form first derived in [35]: $\Psi(k)\sim k^{-3}(1+\lambda k)\exp(-\lambda k)$.

III. ANALYSIS

The time-evolution equation for the spherically integrated scalar covariance spectrum $E(k)=4\pi k^2\Psi(k)$ may be written as

$$\frac{\partial E(k)}{\partial t}=-\frac{\partial \chi(k)}{\partial k}-2Dk^2E(k)+P(k), \tag{14}$$

where $\chi(k)$ is the scalar dissipation rate and $P(k)$ is the production spectrum of scalar variance. Solving for χ in the steady state for the range $k\ll\lambda^{-1}$ gives

$$\chi(k)\approx\chi_0-\int_k^\infty P(\xi)d\xi, \tag{15}$$

where $\chi_0=2D\int_0^\infty k^2E(k)dk$. Equation (15) has been used successfully for incompressible flows where $P=0$ and $\chi(k)=\chi_0$ to determine the constant C_1 in Eq. (13) as a function of $(\chi_0,|\gamma|,\lambda)$, in good agreement with numerical simulations [30,31]. In fact, in the incompressible case χ_0 can be evaluated analytically to give $C_1=\chi_0\lambda^{3/2}/(\pi^{3/2}2\sqrt{2}|\gamma|)$ [35]. For inertial particles ($\sigma\neq0$) the terms in Eq. (6) corresponding to $P(k)$ in Eq. (14) may be easily identified; the covariance production terms are the second term and one-half the third term on the right-hand side (rhs) of Eq. (6). Note that the third term is equal to the sum of the contribution from incompressible advection along compressible streamlines (i.e., spectral transfer) and the contribution from compressible advection along incompressible streamlines (i.e., spectral production). Using Eqs. (9) and (10), it follows that P is given by

$$P(k)=4\pi k^2\frac{10|\gamma|\sigma}{3(1+\sigma)}[6\Psi+k\Psi']. \tag{16}$$

Plots of k vs $P(k)$ with χ_0 set to unity, C_1 calculated numerically from Eq. (15), and Ψ given by Eq. (13) accurate for $k>\eta^{-1}$ are shown as the lines in Fig. 1. The figure reveals that if $P(k)$ is extended to the nonviscous regime $k<\eta^{-1}$, then the extrapolated production of variance due to particle inertia continues to increase with decreasing k. Is this physically reasonable? Consider the term $2\langle\tau b(\mathbf{x})b(\mathbf{y})\rangle\Phi$ in Eq. (6). The correlation function $B(\mathbf{r})=\langle b(\mathbf{x})b(\mathbf{y})\rangle$ has been evaluated in [36] using a quasinormal closure for the fourth-order moments: $B(r)\sim(1215-1080y-198y^2+24y^3+7y^4)\times(1+y)^{-16/3}$ where $y=Gr^2$ and $G=\eta^{-2}30^{-3/2}$. The constant of proportionality follows from $B(r)=30|\gamma|^2\sigma/(1+\sigma)+\cdots$ calculated from Eqs. (9) and (10). The scalar spectrum of the divergence $E^b(k)$ is available in closed form [37]:

$$\begin{aligned}E^b(k)&=\frac{2}{\pi}\int_0^\infty kr\sin krB(r)dr,\\&=\frac{30|\gamma|^2\sigma Hk}{1215(1+\sigma)}[1215k^{29/6}K_{23/6}(kG^{-1/2})+1080e_2\\&\quad-594fe_3-(360f^2+198)e_4+(735f^3-240f)e_5\\&\quad+(735f^2-24)e_6+147fe_7+7e_8],\end{aligned} \tag{17}$$

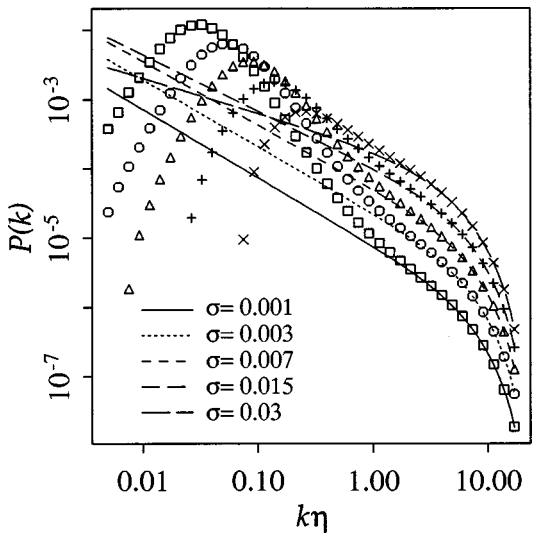

FIG. 1. Log-log plot of the production spectrum of scalar variance for different values of σ. The lines are from Eq. (16) and the symbols from Eq. (22) where the addition of a higher-order term in $F_c(r)$ has produced the correct asymptotic $\lim_{k\to0}P(k)=0$. The parameter values are $\chi_0=1$, $\varepsilon=0.01$, and Pr=1000.

where

$$\begin{aligned}e_n&=(-1)^{n-1}[-k^{29/6}K_{35/6-n}(kG^{-1/2})\\&\quad+(26/3)G^{1/2}k^{23/6}K_{29/6-n}(kG^{-1/2})],\end{aligned}$$

$$f=G^{1/2}/k,$$

and

$$H=\pi^{-3/2}2^{-23/6}\cos(29\pi/6)\Gamma(-13/3)G^{-41/12}.$$

A normalized plot of $E^b(k)$ is shown in Fig. 2. The figure reveals that $E^b(k)$ begins to decrease for k less than about $0.35\eta^{-1}$. However, it is not surprising that a decrease in P below η^{-1} is not observed in Fig. 1 if one considers the truncated form of $B(r)$ used in the calculation of Ψ and P. In

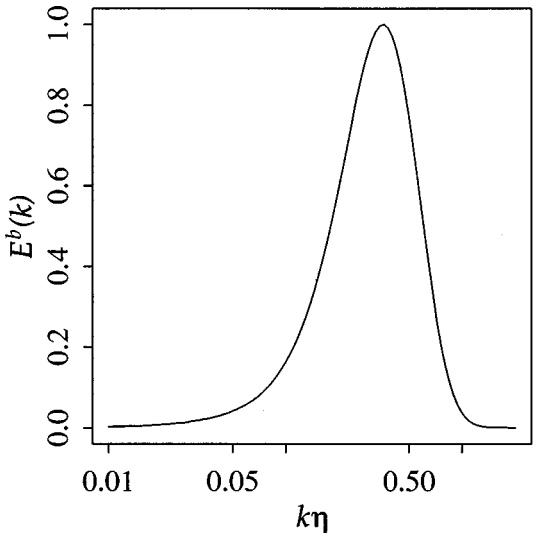

FIG. 2. The scalar spectrum of the velocity divergence from Eq. (17).

fact, calculating $B(r)$ with viscous-regime velocity correlation coefficients (10) gives $B(r)=\text{const}$, which is not particularly accurate for $r>\eta$. In the next section, new expressions for Ψ and P are derived that may be extended to smaller k with greater confidence.

IV. EXTENSION TO LARGER SCALES

The velocity correlation coefficients given in Eq. (10) are the first two terms in a general expansion in even powers of r. Higher-order terms in the F_c expansion, through derivatives F_c' to F_c''', make a significant contribution to $\langle u_m(\mathbf{x})b(\mathbf{y})\rangle$ and $B(r)$. In particular, expanding F_c to the fourth order, $F_c(r)=\epsilon[1-\alpha(r/\eta)^2+\beta\alpha(r/\eta)^4]$, where β is a constant, gives

$$B(r)=\epsilon 30|\gamma|^2\left[1-\frac{14\beta}{3}\left(\frac{r}{\eta}\right)^2\right], \tag{18}$$

which with $\beta=1/154$ well captures the overall behavior of Pinsky *et al.*'s [36] more accurate expression for $B(r)$, and is particularly accurate in the range $r\leqslant 5\eta$ (not shown). The fourth-order term is ignored in $\langle u_m(\mathbf{x})u_n(\mathbf{y})\rangle$ as it makes only a minor contribution in this range. Thus the expressions for both $F(r)$ [Eq. (10)] and $F_c(r)$ are accurate in the $r\leqslant 5\eta$ regime.

Evaluating the contribution of the fourth-order term in F_c with $\beta=1/154$ to the last two terms on the rhs of Eq. (6) and Fourier transforming gives, respectively, two new terms in Eq. (12):

$$\frac{10}{11}\eta^{-2}\frac{\sigma}{1+3\sigma}\Psi''+\frac{4}{11}\eta^{-2}\frac{\sigma}{1+3\sigma}(5\Psi''+k\Psi'''). \tag{19}$$

Writing $\Psi\sim k^{-3}+\delta f(k)$ in the viscous-convective regime (i.e., $E\sim k^{-1}$) and substituting above we find that the second term, compared to the first, is of the order δ and can be ignored. Thus the dominant contribution of the fourth-order term in F_c is through $B(r)$ producing a new equation for Ψ of the form

$$0=(k^2+A^2)\Psi''+Bk\Psi'+C\Psi,$$

where $A=[10/11\eta^{-2}\sigma/(1+3\sigma)]^{1/2}$, B and C are defined as per Eq. (12), and the diffusion term $-\lambda^2k^2\Psi$ of Eq. (12) has been ignored for the range $k\ll\lambda^{-1}$. The substitution $\xi=(1-ik/A)/2$ produces the celebrated hypergeometric equation

$$0=\xi(\xi-1)\Psi''+B(\xi-0.5)\Psi'+C\Psi$$

with solution [34]

$$\Psi=\mathrm{Re}\{C_3\xi^{-a}{}_2F_1(a,a-c+1,a-b+1;\xi^{-1}) + C_4\xi^{-b}{}_2F_1(b,b-c+1,b-a+1;\xi^{-1})\}, \tag{20}$$

where ${}_2F_1\in\mathbb{C}$ is a hypergeometric function, $a=(B-1)/2+[(1-B)^2-4C]^{1/2}/2$, $b=(B-1)/2-[(1-B)^2-4C]^{1/2}/2$, and $c=B/2$. Neither Eq. (12) nor (20) is valid over the whole range of k, and they are in fact related through the asymptotic $\lim_{k\to 0}\Psi$ [Eq. (12)] $=\lim_{k\to\infty}\Psi$ [Eq. (20)]. For Prandtl number $\mathrm{Pr}\gg 1$ (i.e., $\lambda\ll\eta$), there will be a well-defined region near $k=\eta^{-1}$ where these two expressions for Ψ join smoothly. Thus we can write

$$\Psi=\begin{cases} C_1k^{\mu}K_{\nu}(\lambda k), & k\geqslant k_m \\ C_3\,\mathrm{Re}\{\xi^{-a}{}_2F_1(a,a-c+1,a-b+1;\xi^{-1})\}, & k<k_m \end{cases} \tag{21}$$

valid for $\sigma\leqslant 1/27$ where $C_3=\Gamma(\nu)(2A)^{-a}(\lambda/2)^{-\nu}/[2\cos(a\pi/2)]C_1$ and k_m is computed numerically from the intersection $\Psi(k_m)$ [Eq. (12)] $=\Psi(k_m)$ [Eq. (20)].

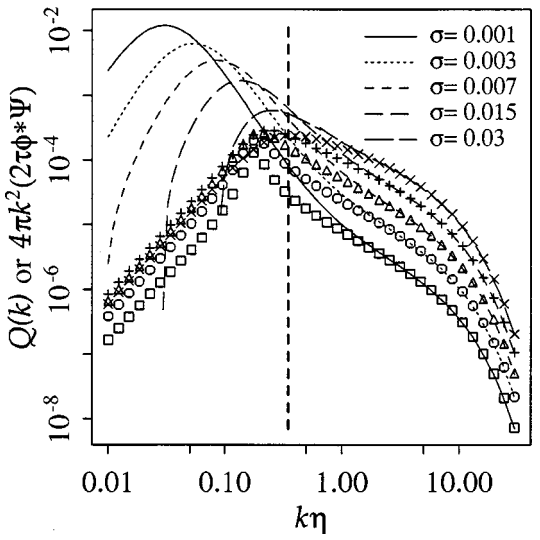

FIG. 3. Comparison of the exact scalar production term $4\pi k^2(2\tau\phi*\Psi)$ (symbols) with the approximation $Q(k)$ (lines). The cutoff used in Eq. (23) at $k=0.35\eta^{-1}$ is shown as a dashed vertical line. For parameter values see Fig. 1.

Incorporating the first term of Eq. (19) into the scalar production spectrum (16) gives

$$P(k)=4\pi k^2\frac{10|\gamma|\sigma}{3(1+\sigma)}\left[6\Psi+k\Psi'+\frac{\Psi''}{11\eta^2}\right]. \tag{22}$$

Plots of k vs $P(k)$ with χ_0 set to unity, C_1 calculated numerically from Eq. (15), and Ψ given by Eq. (21) are shown as the symbols in Fig. 1. The production of scalar variance does, in fact, decrease as $k\to 0$, consistent with $E^b(k)$ shown in Fig. 2. However, the accuracy of $\chi(k)$ determined from $P(k)$ via Eq. (15) in the range $k<\eta^{-1}$ has yet to be determined.

A useful measure of the accuracy of $B(r)$ and hence $P(k)$ can be constructed from the spectral density of the velocity divergence $\phi(k)=E^b(k)/(4\pi k^2)$. The scalar production term $2\langle\tau b(\mathbf{x})b(\mathbf{y})\rangle\Phi$ from Eq. (3) approximated to fourth order using Eq. (18) and Fourier transformed to give $Q(k)=4\pi k^2\{10|\gamma|\sigma/[3(1+\sigma)][3\Psi+\Psi''/(11\eta^2)]\}$ can be compared with the exact expression $4\pi k^2(2\tau\phi*\Psi)$, where $*$ is a spherical convolution. This comparison is shown in Fig. 3 with χ_0 set to unity C_1 calculated numerically from Eq. (15), and ϕ and Ψ given by Eqs. (17) and (21), respectively. Although $Q(k)$ is not equal to the production spectrum $P(k)$—it lacks a contribution from the source term $2\langle\tau u_m(\mathbf{x})b(\mathbf{y})\rangle\partial\Phi/\partial x_m$—a comparison of $P(k)$ in Fig. 1 (symbols) and $Q(k)$ in Fig. 3 (lines) reveals that the two

functions are very similar. Both the approximate and exact source terms shown in Fig. 3 decrease with decreasing k, but clearly $Q(k)$ overestimates the source term in the region $k < \eta^{-1}$. It is therefore appropriate to introduce a cutoff k_c in the evaluation of $\chi(k)$ via Eq. (15) where k_c is defined by

$$\int_{k_c}^{\infty} Q(k) = \int_0^{\infty} 4\pi k^2 (2\tau\phi * \Psi) dk = \frac{10|\gamma|\sigma}{(1+\sigma)} \int_0^{\infty} E(k) dk.$$

For $0 \leqslant \sigma < 1/27$, $k_c = 0.35\eta^{-1}$ suffices with reasonable accuracy and is shown as the dashed vertical line in Fig. 3. Note that this **k**-space cutoff is consistent with the previous statement that the velocity correlation coefficients are accurate in the range $r \leqslant 5\eta$. Equation (15) therefore becomes

$$\chi(k) \approx \chi_0 - \int_{\kappa}^{\infty} P(\xi) d\xi, \quad \kappa = \max(k, 0.35\eta^{-1}). \quad (23)$$

Equations (21)–(23) complete the determination of $\Psi(k)$ as a function of the parameters χ_0, $|\gamma|$, λ, and σ.

V. SPECTRA AND DISCUSSION

Equation (6) for the correlation function $\Phi(r)$ reveals that the covariance of inertial particles is controlled by the competition between radial diffusion $D_{\text{eff}} \nabla_r^2 \Phi$ with positive-definite diffusivity D_{eff}, radial advection $V_{\text{eff}} \partial\Phi/\partial r$ with positive radial velocity $V_{\text{eff}} \sim -\langle \tau u_r(0) b(r) \rangle$, and production Φ/τ_p with time constant $\tau_p^{-1} \sim \langle \tau b(0) b(r) \rangle$. Isotropy and/or parity invariance of the turbulent flow ensures that $D_{\text{eff}} \to D$ and $V_{\text{eff}} \to 0$ at the smallest scales $r \to 0$. Production is maximal at $r = 0$ but the accumulation/rarefaction of particles at such small scales is mitigated by molecular diffusion, which transports the covariance to scales larger than λ. The compressible velocity V_{eff}, which peaks near $r = 10\eta$, always contributes to the transport of particle covariance to larger scales. At near inertial scales, however, D_{eff} begins to dominate both production and ballistic transport, thereby preventing the build up of covariance, i.e., preferential concentration. We can therefore expect preferential concentration to peak near the inertial-viscous subrange transition and this is, in fact, what the present model predicts.

It is unlikely that the production of scalar variance due to particle inertia—limited to small k as shown in Fig. 1—has a large effect on the scaling of the inertial-convective subrange for $\sigma < 1/27$, and, in fact, simulations of massless particles in low-Mach number compressible turbulence show little variation in scaling for $\sigma = 1$ [38]. Numerical simulations [30,31] of the viscous-convective subrange for incompressible flow $\sigma = 0$ suggest that the scale break k_b between the inertial- and viscous-convective subranges occurs, naturally, at the intersection between the inertial-convective spectrum $E_{ic}(k) = C_{ic}\chi_{ic}\varepsilon^{-1/3}k^{-5/3}$ and $E(k): E_{ic}(k_b) = E(k_b)$ where $C_{ic} \approx 3/4$ is the Obukhov-Corrsin constant, ε is the energy dissipation rate, and $\chi_{ic} \equiv \chi(k_b) = \text{const}$ is the inertial-convective range scalar dissipation rate. For $\sigma = 0$, $\chi_{ic} = \chi_0$ and the scale break is given by $k_b = (C_{ic}/q)^{3/2}\eta^{-1} \approx 0.05\eta^{-1}$ where q is a function of $|\gamma|$, whereas for $\sigma \neq 0$, χ_{ic} decreases with increasing σ according to Eq. (23). However, for purposes of comparison, it is convenient to set $\chi_{ic}(\sigma)$ to a constant reference value, i.e., unity. The scalar dissipation in the viscous-convective range is therefore $\chi_{vc}(k,\sigma) = \chi(k,\sigma)\chi_{ic}/\chi(k_b,\sigma)$, which increases with increasing σ.

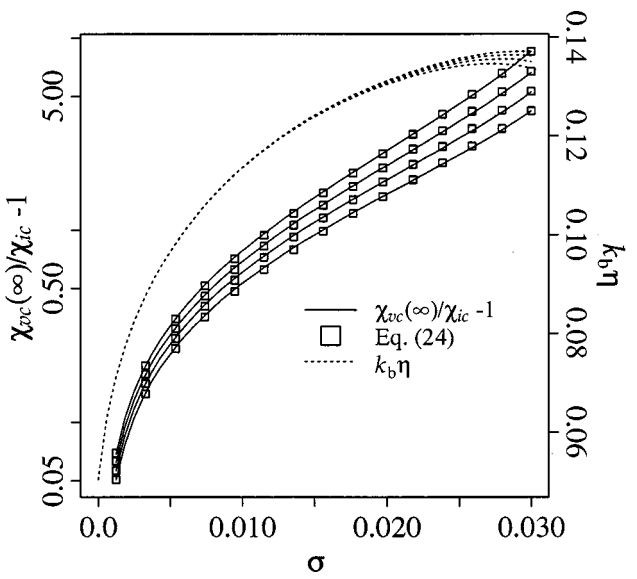

FIG. 4. Plot showing both the scale break k_b (right axis) between the $k^{-5/3}$ inertial-convective subrange and the viscous-convective subrange, and the measure of self-excitation $\chi_{vc}(\infty,\sigma)/\chi_{ic} - 1$ (left axis) computed numerically (lines) and approximated analytically by Eq. (24) (□). These functions have been calculated using model (21)–(23) at four Prandtl numbers and appear such that the lines are, from top to bottom, Pr = 8000, 3000, 1200, and 500.

The scale break k_b shown in Fig. 4 has been computed numerically using model (21)–(23) and the inertial-convective range spectrum (above) for Pr in the range 500 – 8000. Also shown is a measure of the increase in scalar dissipation rate through the viscous-convective regime $\chi_{vc}(\infty,\sigma)/\chi_{ic} - 1$. The figure illustrates a number of robust trends that are worthy of discussion. First, k_b increases from $\approx 0.05\eta^{-1}$ at $\sigma = 0$ to $\approx 0.135\eta^{-1}$ near $\sigma = 0.03$; the viscous-convective regime gets pushed to smaller scales. Thus as σ increases, the accuracy of the entire modeled inertial-convective/viscous-convective spectrum also increases, under the assumption that the scaling $E_{ic} \sim k^{-5/3}$ remains invariant. Second, and as mentioned above, $\chi_{vc}(\infty)$ increases with increasing σ. To aid in this discussion, $\chi_{vc}(\infty)$ has been fit to the approximate analytic form

$$\chi_{vc}(\infty) \approx \chi_{ic} \exp[\ln(\text{Pr})^{0.85}(8.5\sigma + 3480\sigma^3)], \quad (24)$$

depicted with □ in Fig. 4. This equation demonstrates, formally, the self-excitation (exponential growth) in the second moment of particle concentration first discussed in [18]. The weak Pr dependence results from a ''longer'' viscous-convective regime with increasing Pr and therefore more self-excitation. Self-excitation begins near $\sigma \approx 0.04 \ln(\text{Pr})^{-0.85}$ and along with self-excitation of higher-order moments leads to preferential concentration.

The scalar spectrum E, computed numerically using model (21)–(23) and the inertial-convective range spectrum, is shown in Fig. 5 along with the change in scalar dissipation rate $\chi_{vc}(k)/\chi_{ic}$. Both features discussed above—the sup-

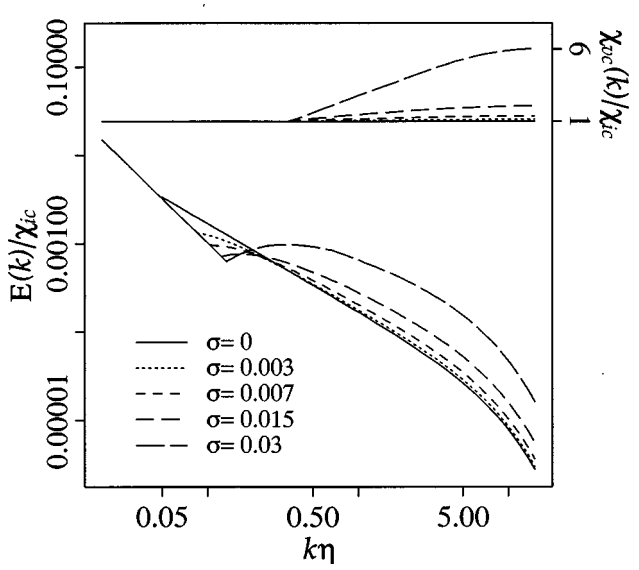

FIG. 5. The scalar spectrum computed at various σ using model (21)–(23) and the corresponding increase in scalar dissipation rate. Note that the increase in χ_{vc} begins at $k=0.35\eta^{-1}$ as per Eq. (23). The parameter values are $\varepsilon=0.01$ and Pr$=1000$.

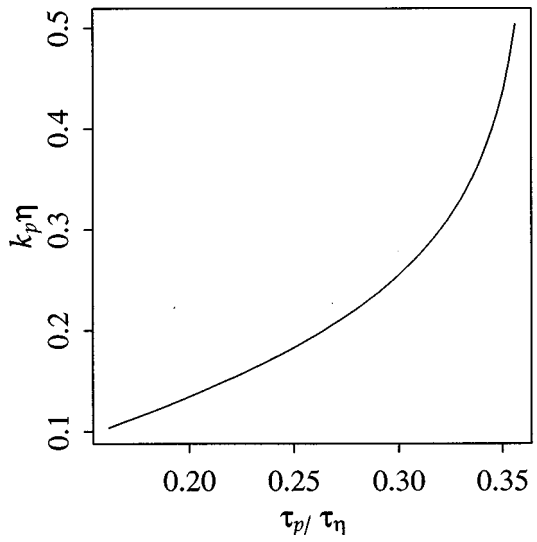

FIG. 6. Plot showing the characteristic scale of preferential concentration as a function of the Stokes number. The wave number k_p is computed from $\partial E/\partial k|_{k_p}=0$ using model (21)–(23).

pression of the viscous-convective regime at larger scales and the self-excitation of the spectrum—are clearly visible. Beginning at $\sigma\approx 0.007$, a peak at $k_p\approx 0.1\eta^{-1}$ is visible in the spectrum and becomes more pronounced as σ increases. The wave number k_p is a useful measure of the length scale at which preferential concentration occurs, and it is discussed further below.

An important parameter in most studies of preferential concentration in the literature is the Stokes number, which plays a role similar to ϵ (or σ) in this work. The Stokes number is usually defined as the ratio τ_p/τ_η where τ_p is the particle aerodynamic time constant [20]. Comparing Eq. (18) to Pinsky *et al.* [36] expression $B(r)=(4/15)\tau_p^2/\tau_\eta^4+\cdots$ gives

$$\epsilon=\frac{4}{15}\left(\frac{\tau_p}{\tau_\eta}\right)^2. \tag{25}$$

The wave number of the spectral peak k_p defined by $\partial E/\partial k|_{k_p}=0$ is plotted as a function of the Stokes number τ_p/τ_η in Fig. 6 in the range $0.007<\sigma<1/27$ corresponding roughly to $0.15<\tau_p/\tau_\eta<0.35$. The figure reveals that the characteristic scale of preferential concentration increases from $\approx 60\eta$ at a Stokes number of 0.15 to $\approx 13\eta$ at a Stokes number of 0.35, consistent with the estimate in [20] that particles with a Stokes number of around 1 are concentrated at length scales $(6–20)\eta$. Note also that rapid growth in the viscous-convective regime for Stokes numbers greater that 0.15 ($\sigma>0.007$) shown in Fig. 5 is consistent with the rapid growth in preferential concentration in the range of Stokes numbers 0.2–1 shown in Fig. 18 of [21].

VI. CONCLUSIONS

The effect of particle inertia on the viscous-convective subrange has been investigated for $\sigma\leqslant 1/27$ (small Stokes number regime). Using the δ-correlated model, an analytic expression for the second-order spectral density of inertial particles is derived as a function of a Batchelor-type diffusive length scale, the rate of strain of Kolmogorov eddies, the scalar dissipation rate, and the degree of compressibility (Stokes number). A rich spectral behavior is observed in the viscous-convective regime that includes the following features. Particle inertia suppresses small k viscous-convective scaling; the start of the viscous-convective regime is pushed to smaller scales with increasing σ, beginning near $k\approx 0.135\eta^{-1}$ for $0.02<\sigma<1/27$ (Stokes numbers ≈ 0.3). Associated with increased compressibility is the emergence of a well-defined ''bump'' in the spectrum beginning at a $\sigma\approx 0.007$ (Stokes number ≈ 0.15). The bump represents the accumulation of inertial particles in regions of high strain and low vorticity in the flow and is a manifestation of intermittency in the spatial statistics. The characteristic scale of this preferential concentration ranges from around 60η at $\sigma=0.007$ (Stokes number$=0.15$) to about 13η at $\sigma=1/27$ (Stokes number$=0.35$). The relative height of the bump increases exponentially with an increasing Stokes number, consistent with results from numerical simulations [21] that show a rapid increase in preferential concentration with an increasing Stokes number for Stokes numbers less than unity.

ACKNOWLEDGMENTS

I am grateful to Phillip Austin and Nicole Jeffery for a careful reading of the manuscript. I also thank Tov Elperin for a useful discussion. This work is supported by the Natural Sciences and Engineering Research Council of Canada.

[1] Y. B. Zeldovich, S. A. Molchanov, A. A. Ruzmaikin, and D. D. Sokoloff, Sov. Sci. Rev. C. Math. Phys. **7**, 1 (1988).
[2] M. Avellaneda and A. J. Majda, Philos. Trans. R. Soc. London, Ser. A **346**, 205 (1994).
[3] V. I. Klyatskin, Usp. Fiz. Nauk **164**, 531 (1994) [Phys. Usp. **37**, 501 (1994)].
[4] K. Gawedzki and A. Kupiainen, in *Low-Dimensional Models in Statistical Physics and Quantum Field Theory*, edited by H. Gross and L. Pittner (Lecture Notes in Physics Vol. 469) (Springer-Verlag, Berlin, 1996), pp 71–105.
[5] L. I. Piterbarg and A. G. Ostrovskii, *Advection and Diffusion in Random Media. Implications for Sea Surface Temperature Anomalies* (Kluwer Academic Publishers, Dordrecht, 1997).
[6] T. Komorowski, Stoch. Process. Their Appl. **74**, 165 (1998).
[7] R. H. Kraichnan, Phys. Rev. Lett. **72**, 1016 (1994).
[8] R. H. Kraichnan, V. Yakhot, and S. Chen, Phys. Rev. Lett. **75**, 240 (1995).
[9] A. J. Majda and P. R. Kramer, Phys. Rep. **314**, 238 (1999).
[10] A. L. Fairhall, O. Gat, V. Lvov, and I. Procaccia, Phys. Rev. E **53**, 3518 (1996).
[11] M. Chertkov, G. Falkovich, and V. Lebedev, Phys. Rev. Lett. **76**, 3707 (1996).
[12] L. T. Adzhemyan, N. V. Antonov, and A. N. Vasil'ev, Phys. Rev. E **58**, 1823 (1998).
[13] V. I. Belinicher, V. S. L'vov, A. Pomyalov, and I. Procaccia, J. Stat. Phys. **93**, 797 (1998).
[14] O. Gat, V. S. Lvov, and I. Procaccia, Phys. Rev. E **56**, 406 (1997).
[15] B. I. Shraiman and E. D. Siggia, Phys. Rev. E **57**, 2965 (1998).
[16] T. Elperin, N. Kleeorin, and I. Rogachevskii, Phys. Rev. E **52**, 2617 (1995).
[17] L. T. Adzhemyan and N. V. Antonov, Phys. Rev. E **58**, 7381 (1998).
[18] T. Elperin, N. Kleeorin, and I. Rogachevskii, Phys. Rev. Lett. **77**, 5373 (1996).
[19] T. Elperin, N. Kleeorin, and I. Rogachevskii, Phys. Rev. E **58**, 3113 (1998).
[20] J. K. Eaton and J. R. Fessler, Int. J. Multiphase Flow Suppl. **20**, 169 (1994).
[21] L.-P. Wang and M. R. Maxey, J. Fluid Mech. **256**, 27 (1993).
[22] L. F. Richardson, Proc. R. Soc. London, Ser. A **110**, 709 (1926).
[23] Y. B. Zel'dovich, Zh. Eksp. Teor. Fiz. **7**, 1466 (1937).
[24] P. H. Roberts, J. Fluid Mech. **11**, 257 (1961).
[25] R. Kubo, J. Math. Phys. **4**, 174 (1963).
[26] R. H. Kraichnan, Phys. Fluids **11**, 945 (1968).
[27] R. A. Carmona and J. P. Fouque, *Seminar on Stochastic Analysis, Random Fields and Applications*, Vol. 36 of *Progress in Probability* (Birkhäuser Verlag, Basel, 1995), pp. 37–49.
[28] L. Piterbarg, *Stochastic Models in Geosystems* MA Volumes in Mathematics and its Applications Vol. 85 (Springer-Verlag, Berlin, 1997), pp. 313–352.
[29] G. K. Batchelor, J. Fluid Mech. **5**, 113 (1959).
[30] D. Bogucki, J. A. Domaradzki, and P. K. Yeung, J. Fluid Mech. **343**, 111 (1997).
[31] J. R. Chasnov, Phys. Fluids **10**, 1191 (1998).
[32] T. Elperin, N. Kleeorin, and I. Rogachevskii, Phys. Rev. Lett. **76**, 224 (1996).
[33] A. S. Monin and A. M. Yaglom, *Statistical Fluid Mechanics: Mechanics of Turbulence* (MIT Press, Cambridge, MA, 1975), Vol. 2.
[34] *Handbook of Mathematical Functions*, edited by M. Abramowitz and I. A. Stegun (Dover, New York, 1970).
[35] R. C. Mjolsness, Phys. Fluids **18**, 1393 (1975).
[36] M. B. Pinsky, A. P. Khain, and Z. Levin, Q. J. R. Meteorol. Soc. **125**, 553 (1999).
[37] L. Sirovich, L. Smith, and V. Yakhot, Phys. Rev. Lett. **72**, 344 (1994); see also **74**, 1492(E) (1995).
[38] X. D. Cai, E. E. O'Brien, and F. Ladeinde, Phys. Fluids **10**, 2249 (1998).